Anuário do Instituto de Geociências
Universidade Federal do Rio de Janeiro
https://revistas.ufrj.br/index.php/aigeo/

ISSN 0101-9759
e-ISSN 1982-3908

GEOLOGY

Petrogenesis of Cambro-Ordovician Magmatism in Araçuaí Orogen, SE Brazil: Petrography, Litogeochemistry and Zircon Geochronology of the Pedra Azul Intrusive Complex

Petrogênese do Magmatismo Cambro-Ordoviciano no Orógeno Araçuaí, SE do Brasil: Petrografia, Litogeoquímica e Geocronologia de Zircão do Complexo Intrusivo Pedra Azul

Iago Mateus Lopes de Macêdo[1]; Guilherme Loriato Potratz[2]; Marilane Gonzaga de Melo[3]; Rodson de Abreu Marques[4]; Camila Cardoso Nogueira[2]; Werlem Holanda dos Santos[2]; Renzo Dias Rodrigues[5]; Mauro Cesar Geraldes[2]

[1] Universidade do Estado do Rio de Janeiro, Faculdade de Geologia, Programa de Pós-Graduação em Geociências, Rio de Janeiro, RJ, Brasil
[2] Universidade do Estado do Rio de Janeiro, Faculdade de Geologia, Departamento de Mineralogia e Petrologia Ígnea, Rio de Janeiro, RJ, Brasil
[3] Universidade Federal do Espírito Santo, Centro de Ciências Exatas, Naturais e da Saúde, Departamento de Geologia, Alegre, ES, Brasil
[4] Universidade Federal de Ouro Preto, Escola de Minas, Departamento de Geologia, Ouro Preto, MG, Brasil.
[7] Universidade do Estado do Rio de Janeiro, Faculdade de Geologia, Programa de Pós-Graduação em Geociências, Rio de Janeiro, RJ, Brasil

E-mails: lopes.iago1@gmail.com; geo.loriato@gmail.com; marilanegonzaga@hotmail.com; rodsonabreu@gmail.com; cnogueiracamila@gmail.com; werlemholanda@gmail.com; renzorodrigues18@gmail.com; mauro.geraldes@gmail.com

Abstract

The Araçuaí Orogen is characterized by intense magmatic activity corresponding to pre-, syn-, and post-tectonic evolutionary stages between the Neoproterozoic and the Cambro-Ordovician. Bimodal plutons predominantly mark the final stage of this magmatism. The Pedra Azul Intrusive Complex (PAIC) is a post-collisional pluton composed of rocks ranging from syenogranite and monzogranite (featuring ocellar textures) to granodiorite, tonalite and quartz-monzodiorite. The PAIC was emplaced along a regional lineament during the orogen's collapse phase, intruding metasedimentary sequences, which are observed as xenoliths and roof pendants within the granites of the intrusion. This study presents detailed petrographic analyses, combined with lithogeochemical data and zircon U-Pb geochronology. Macro- and micro-scale evidence indicates that the lithotypes within the PAIC interacted to produce mixing and mingling features. Geochemical data divide the mapped rocks of the PAIC into three distinct groups: granite group, intermediary group, and ocellar granite. Magma mixing modeling demonstrated that binary mixing between granites and intermediary rocks corresponds to the composition of the ocellar granites. U-Pb zircon dating (via laser ablation inductively coupled plasma mass spectrometry [LA-ICP- MS]) revealed crystallization ages of 501 ± 5 Ma for monozogranite and 505 ± 3 Ma for syenogranite, 494 ± 4 Ma, 486 ± 5 Ma and 497 ± 3 Ma for granodiorite, and 503 ± 3 Ma for tonalite. The data obtained for the PAIC indicate that the rocks composing the complex were formed from different sources.

Keywords: Two-component mixture; Hybridization of granitoids; Crustal melting

Resumo

O Orógeno Araçuaí é marcado por intensa atividade magmática correspondente aos estágios evolutivos pré-sin- e pós-tectônico entre o Neoproterozoico e o Cambro-Ordoviciano. O estágio final desse magmatismo tem como característica principal plútons bimodais. O Complexo Intrusivo Pedra Azul (PAIC) é um plúton pós-colisional composto por rochas que variam de sienogranito e monzogranito (que apresentam texturas ocelares), granodiorito, tonalito e quartzo-monzodiorito. O PAIC foi intrudido ao longo de um lineamento regional na fase de colapso do orógeno, intrudindo sequências metassedimentares, que são observadas como xenólitos e *roof pedants* nos granitos da intrusão. Neste trabalho, são apresentados estudos

Received: 24 December 2024; Accepted: 21 June 2025

detalhados de petrografia, associados a dados litogeoquímica e geocronologia U-Pb em zircão. Evidências em macro e microescala mostram que os litotipos presentes no PAIC demonstram interação gerando produtos de mixing e mingling. Os dados geoquímicos dividem as rochas mapeadas no PAIC em três grupos distintos, um grupo granítico, outro intermediário e por fim de granito ocelar. A modelagem de mistura de magmas demonstrou que a mistura binária entre granitos e o grupo intermediário corresponderia à composição dos granitos ocelares. A datação por U-Pb em zircões (por ablação a laser - espectrometria de massa com plasma indutivamente acoplado (LA-ICP-MS)) revelam idades de cristalização de 501 ± 5 Ma para monzogranito e 505 ± 3 Ma para sienogranito, 494 ± 4 Ma, 486 ± 5 Ma e 497 ± 3 Ma para granodiorito e 503 ± 3 Ma para tonalito. Os dados obtidos para o PAIC indicam que as rochas que o compõe foram formadas por diferentes fontes.

Palavras-chave: Mistura de dois componentes; Hibridização de granitoides; Fusão Crustal

1 Introduction

The end of an orogenic cycle is marked by lithospheric extension and asthenospheric mantle upwelling during the collapse stage, leading to crust-mantle interaction through intense magmatic activity, crustal anatexis, and metamorphism (Dewey 1998; Liégeois *et al.* 1998; Niu *et al.* 2013; Sami *et al.* 2018; Song *et al.* 2015). Post-collisional magmatism provides critical geodynamic and petrogenetic insights into the evolution of orogenic belts, such as information on the end of collision and extensional collapse, crustal growth and reworking, mantle processes, and crust-mantle interaction (Gómez-Frutos, Castro & Gutiérrez-Alonso 2023; Sengor *et al.* 2008; Wang *et al.* 2014; Yang *et al.* 2019).

The tectonic evolution of an orogen is primarily marked by changes in magmatic composition (Bonin 2004; Harris, Pearce & Tindle 1986). The Araçuaí Orogen, as described by Alkmim *et al.* (2006, 2007), is an orogenic system located in southeastern Brazil, spanning the states of Espírito Santo and Minas Gerais. It records a long evolutionary history, characterized by extensive magmatism ranging from the Neoproterozoic to the Ordovician, divided into different evolutionary stages that have been intensively studied over the past two decades (Araujo *et al.* 2020, 2023; De Campos *et al.* 2004, 2016; Gonçalves *et al.* 2014, 2016, 2018; Melo *et al.* 2017a, 2017b;

Pedrosa-Soares *et al.* 2007, 2011, 2020; Santiago *et al.* 2020, 2023; Serrano *et al.* 2018; Tedeschi *et al.* 2016; Wiedemann *et al.* 2002).

The post-collisional period of the Araçuaí Orogen is characterized by intense magmatic activity between 530 and 480 Ma, forming elongated and circular plutons with a broad compositional spectrum ranging from gabbro/norite to syenogranite, along with various well-documented magma mixing features (Aranda *et al.* 2020; Araujo *et al.* 2020; De Campos *et al.* 2016; Ludka & Wiedemann-Leonardos, 2000; Macêdo *et al.* 2022; Medeiros, Wiedeman-Leonardos & Mendes 2001; Mendes & De Campos, 2012; Serrano *et al.* 2018;Wiedemann *et al.* 2002). The Pedra Azul Intrusive Complex (PAIC), located in the southern region of Espírito Santo state, represents this stage in the evolutionary history of the Araçuaí Orogen, exhibiting rocks of varying compositions, magma mixing features, and an absence of deformation (Araujo *et al.* 2020; De Campos *et al.* 2004, 2016).

Although isotopic, geochronological, and magnetic susceptibility anisotropy studies (emplacement) have been the primary methods for investigating the genesis and evolution of igneous bodies over the past decade, petrographic and geochemical studies still provide valuable information regarding magmatic processes. Therefore, this study aims to present new petrographic, lithogeochemical, and zircon U-Pb geochronological data of the PAIC, discuss and characterize the associated magmatic processes, and to bring new insights into the evolution of this suite within the context of the Araçuaí Orogen.

2 Geological Setting

The Araçuaí Orogen (Figure 1), spanning from the Neoproterozoic to the Ordovician, represents the northern segment of the Mantiqueira Province and is associated with the formation of the West Gondwana supercontinent (Pedrosa-Soares *et al.* 2020; Santiago *et al.* 2020; Soares *et al.* 2020; Tedeschi *et al.* 2016). It borders the São Francisco Craton to the north and west, the Atlantic Margin to the east, and the Ribeira Orogen to the south, forming part of the Araçuaí-Ribeira Orogenic System (AROS) (Heilbron *et al.* 2004; Santiago *et al.* 2020; Tedeschi *et al.* 2016).

The Araçuaí and Western Congo orogens form a confined orogen between the São Francisco and Congo cratons, with its tectonic evolution described by the Wilson Cycle (1966): precursor basin, rift, passive margin, ocean formation and closure, and post-collisional collapse (Caxito *et al.* 2022; Kuchenbecker *et al.* 2015; Pedrosa- Soares *et al.* 2011; Queiroga *et al.* 2007; Tedeschi *et al.* 2016). Its basement includes Archean and Paleoproterozoic rocks, granulites, granitoids, and migmatitic gneisses from various complexes, as well as supracrustal rocks such as greenstone belts and metavolcanosedimentary sequences (Alkmim *et al.* 2017; Degler *et al.* 2018; Gonçalves *et al.* 2014). The Macaúbas Group, representing the precursor basin, includes metamorphosed mafic to ultramafic rocks, remnants of oceanic crust (Amaral *et al.* 2020; Babinski *et al.* 2012; Kuchenbecker *et al.* 2015; Pedrosa-Soares *et al.* 2001; Queiroga *et al.* 2007).

The pre-collisional stage (630–585 Ma) marks the closure of the Macaúbas Basin, the formation of the Rio Doce magmatic arc, and the G1 Supersuite, with calc-alkaline compositions including dioritic autoliths and gabbroic bodies (Noce *et al.* 2004; Pedrosa-Soares *et al.* 2011; Santiago *et al.* 2022; Soares *et al.* 2020; Tedeschi *et al.* 2016). Passive margins are represented by metamorphosed complexes such as Nova Venécia and Jequitinhonha (Alkmim *et al.* 2006; Araujo *et al.* 2023; Gradim *et al.* 2014; Richter *et al.* 2016; Santiago *et al.* 2023).

The syn-collisional granitogenesis (585–560 Ma), corresponding to the G2 Supersuite, produced aluminous garnet-rich granites, marking the peak of metamorphism. Between 560–530 Ma, the G3 Supersuite generated leucogranites derived from autochthonous/parautochthonous melting (De Campos *et al.* 2004, 2016; Gradim *et al.* 2014; Melo *et al.* 2017a, 2017b; Pedrosa-Soares *et al.* 2011; Serrano *et al.* 2018; Tedeschi *et al.* 2016). The post-collisional stage (530–480 Ma) produced the G4 and G5 supersuites, characterized by plutons ranging from olivine gabbro to syenogranite, as well as features of magmatic hybridization (Bellon *et al.* 2022; De Campos *et al.* 2004, 2016; Macêdo *et al.* 2022; Potratz *et al.* 2022; Serrano *et al.* 2018; Teixeira *et al.* 2020; Wiedemann- Leonardos *et al.* 2002; Zanon *et al.* 2015).

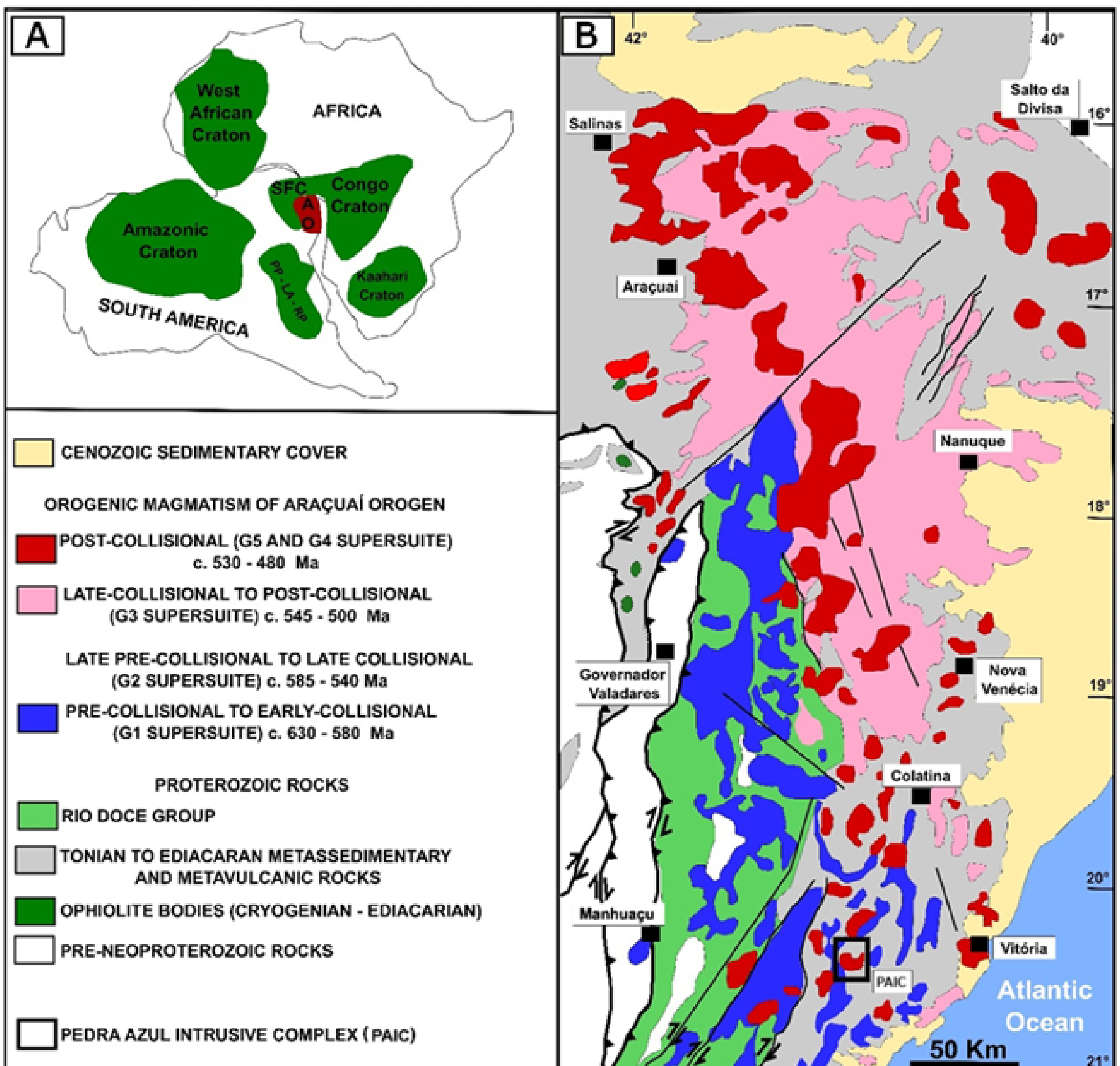

Figure 1 A. Araçuaí–Western Congo Orogenic System and adjacent cratonic regions in the context of the West Gondwana supercontinent (Modified from Alkmim *et al.* 2006); B. Simplified geological map of the Araçuaí Orogen (modified from Pedrosa-Soares *et al.* 2011), showing the location of the Pedra Azul Intrusive Complex.

3 Materials and Methods

The samples collected in the field were processed at the Geological Sample Processing Laboratory (LGPA) of the Rio de Janeiro State University (UERJ), where 30 thin sections were prepared for the PAIC samples. These sections were subsequently analyzed at the Petrography Laboratory of the Faculty of Geology at UERJ. For geochemical analysis, the freshest and most homogeneous samples were selected. Major oxides were analyzed in whole rock using lithium borate fusion and XRF determination. Trace elements were analyzed in whole rock via digestion in aqua regia or using a four-acid combination determined by ICP-MS. The analyses were performed at the ALS laboratory.

Six samples from the PAIC were collected for U-Pb age determination. Sample preparation for geochronology was carried out at the LGPA of UERJ. The samples were washed, manually reduced using a hammer and an anvil, crushed with a jaw crusher, and milled with a disc mill. The pulverized material underwent density separation processes, beginning with a hydrodynamic separation table, followed by separation using dense liquids (iodine and bromoform). Finally, concentrates were subjected to magnetic separation (Frantz) and manual picking.

Subsequent U-Pb zircon analyses were performed at the Multi-user Environmental Laboratory (MultiLab) at UERJ, using a Laser Ablation Inductively Coupled Plasma Mass Spectrometer (LA-ICP-MS) equipped with an Element-2 spectrometer. The data acquisition sequence on the equipment was as follows: (1) blank reading; (2) GJ-1 standard reading; (3) sequential reading of nine unknown grains; (4) 91,500 standard reading; (5) GJ-1 standard reading; (6) blank reading. Ablation of the grain surfaces was performed using laser pulses with a 30 μm diameter, and the vaporized material was transported in Ar (0.80 L/min) and He (0.55 L/min) for analysis using 700 cycles of 1’1’’ each. The analyses included measurements of ^{204}Pb, ^{206}Pb, ^{207}Pb, ^{208}Pb, ^{232}Th, and ^{238}U masses. Hg is a common contaminant in He and Ar gases, and the ^{204}Hg mass interferes with the ^{204}Pb mass counts. Therefore, the ^{202}Hg mass count was used to correct this isobaric interference.

The samples were analyzed alongside zircon standards GJ-1 (normalization TIMS data: ^{207}Pb/^{206}Pb = 608.3 Ma, ^{206}Pb/^{238}U = 600.7 Ma, and ^{207}Pb/^{235}U = 602.2 Ma) (Jackson, Pearson & Griffin 2004) and 91,500 (ID-TIMS age for ^{206}Pb/^{238}U = 1,062.4 ± 0.8 Ma and ^{207}Pb/^{206}Pb = 1,065.4 ± 0.6 Ma).

4 Results

4.1 Field Aspects and Petrography

The Pedra Azul Intrusive Complex (PAIC) spans an area of approximately 200 km². PAIC rocks crop out in slabs, road cuts, quarries, waterfalls, blocks, and boulders. The PAIC is composed of rocks with varying compositions, including monzogranite, syenogranite, granodiorite, tonalite and quartz-monzodiorite (Figure 2). The QAPF diagram and modal composition results are presented in Supplementary Material 1.

Topographic contrast is a characteristic feature of the PAIC; however, it differs from other post-collisional plutons in the region, such as the Castelo and Venda Nova Intrusive Complexes, located near the PAIC. In the PAIC, the core is granitic and represents the highest elevations in the region (Blue Stone Peak and Flowers Peak) (Figure 3A). Granodiorite and tonalite occur between the granitic core and the border of the massif. Ocellar granite and quartz monzodiorite are restricted to the northern and eastern portions of the PAIC.

Two metasedimentary units host the PAIC: biotite-sillimanite gneiss to the west and quartzites to the east of the massif. The biotite-sillimanite gneiss has fine grain size and granoblastic texture, with a mineral composition of feldspar, quartz, sillimanite, and biotite. Migmatization zones are occasionally observed, as seen near Aracê, where interdigitation with small granitic and pegmatitic intrusions into the paragneiss occurs. The quartzite is white, predominantly composed of quartz, with irregularly arranged mafic bands and fine grain size. Its mineralogy includes quartz, biotite, feldspar, titanite, and, in some cases, tourmaline. Contacts with PAIC rocks are low angle, often containing xenoliths or roof pendants of host rocks within the marginal granite (Figure 3B).

The Pedra Azul Intrusive Complex (PAIC) is a heterogeneous intrusion, where syenogranite and monzogranite occur both at the margins and in the core, making field separation challenging. On the northern and eastern margins of the massif, ocellar granite is observed, consisting of felsic spots approximately 5 cm in size within a biotite-rich matrix, with compositions ranging from syenogranite to monzogranite (Figure 3D). These rocks are leucocratic, with seriate inequigranular textures and fine- to coarse-grained sizes. Granodiorite and tonalite occur between the margins and the core, exhibiting medium grain size and an inequigranular texture, as well as features related

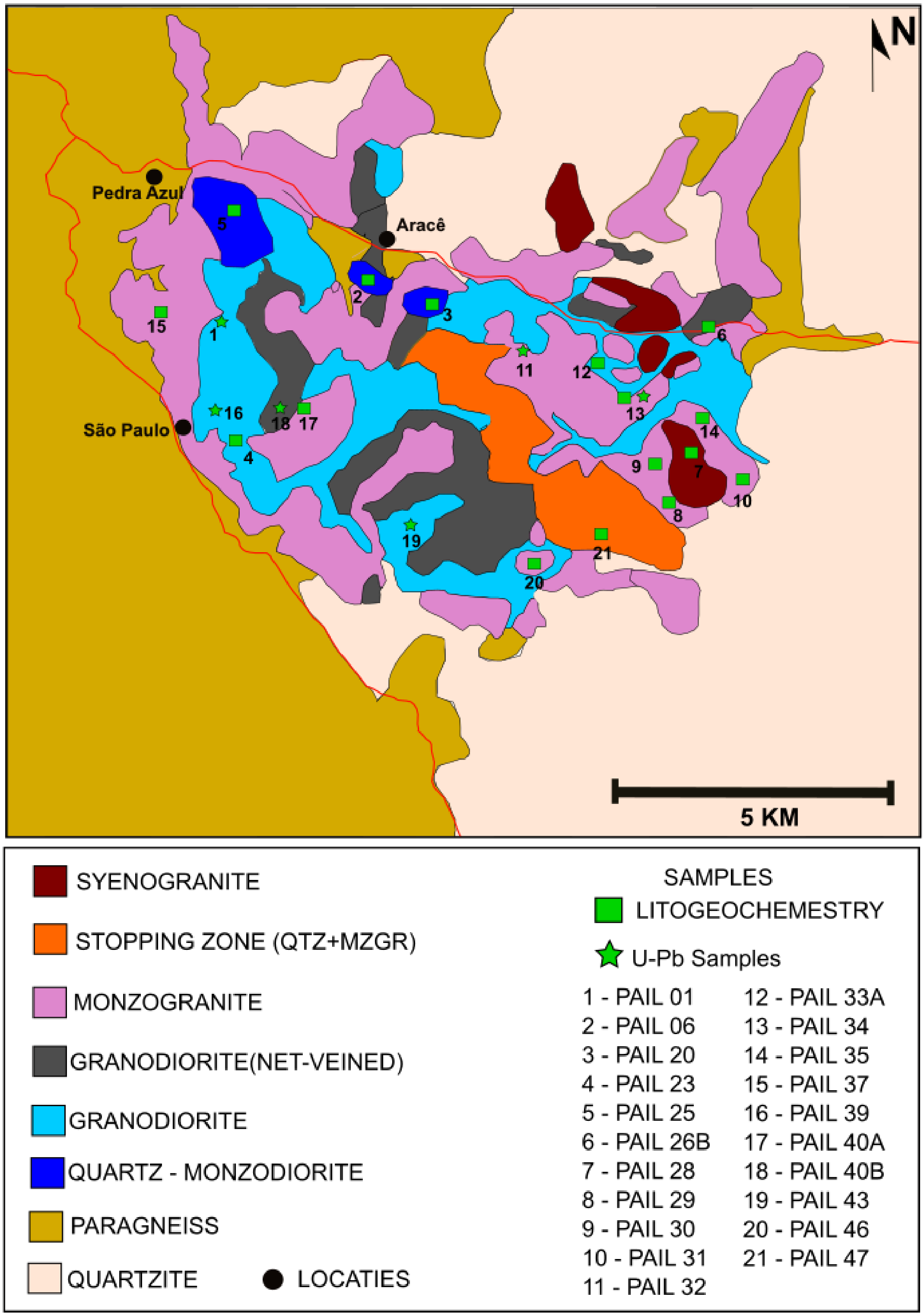

Figure 2 Geological map of the Pedra Azul Intrusive Complex (modified from Costa de Moura *et al.* 1997). Green rectangles indicate sampling locations for lithogeochemical analyses, while green stars represent sampling locations for U-Pb geochronology. Legends (rectangles and stars): 1-PAIL 01; 2-PAIL 06; 3-PAIL 20; 4-PAIL 23; 5-PAIL 25; 6-PAIL 26B; 7-PAIL 28; 8-PAIL 29; 9-PAIL 30; 10-PAIL 31; 11-PAIL 32; 12-PAIL 33A; 13-PAIL 34; 14-PAIL 35; 15-PAIL 37; 16-PAIL 39; 17-PAIL 40A; 18-PAIL 40B; 19-PAIL 43; 20-PAIL 46; 21-PAIL 47.

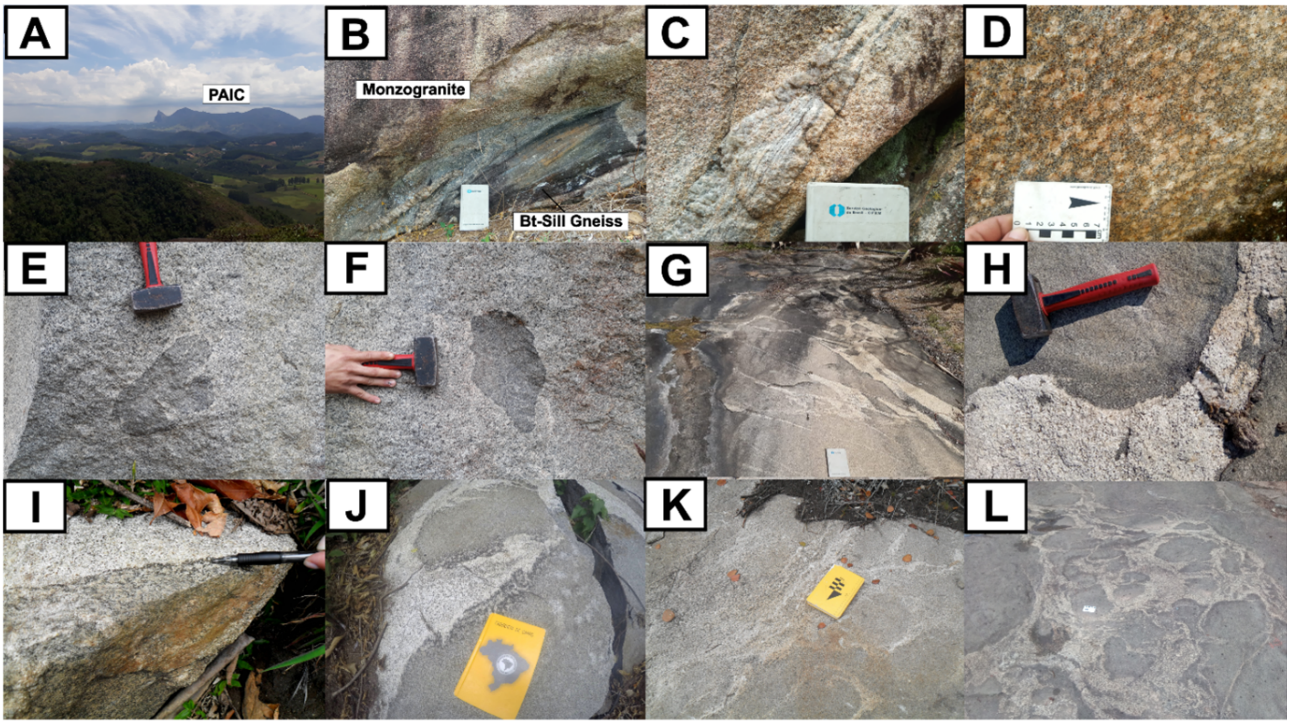

Figure 3 A. The Pedra Azul Intrusive Complex seen from a distance, showcasing its steep relief with a granitic core; B. Xenoliths of biotite-sillimanite paragneiss within the marginal monzogranite; C. Pegmatitic dike cutting the monzogranite; D. Ocellar granite with quartz and feldspar ocelli; E-F. Mafic microgranular enclave within granite; G. Outcrop of granodiorite with net-veined granitic intrusions; H-I. Chilled margins at the contact between quartz-monzonite and a granitic pocket; J-K. Hybrid zone observed at the contact between granodiorite and a granitic pocket in the Pedra Azul State Park; L. Pillow-like structure marked by quartz-monzodiorite enclaves into a granitic rock.

to magma mixing. Finally, quartz monzodiorite occurs in the northern portion of the massif, showing dark color, fine grain size, equigranular texture, and several features associated with magma mixing.

Throughout the complex, pegmatitic dikes (Figure 3C), fractures, mafic dikes, and quartz veins are common. Mafic microgranular enclaves are also observed, varying in size, shape, and color, and frequently exhibiting a “salt-and- pepper” texture (Figures 3E and 3F). Magma mixing features are frequent in this area, such as net-veined intrusions (Figure 3G), chilled margins (Figures 3H and 3I), hybridization zones at contacts between contrasting lithotypes (Figures 3J and 3K), and pillow-like features where granitic venules enclose host rocks (Figure 3L).

Microscopically, the rocks of the PAIC do not show significant mineralogical variation, displaying only differences in mineral proportions. Microcline occurs predominantly in the monzogranite and syenogranite, in smaller amounts in the granodiorite, and is not observed in the tonalite and quartz monzodiorite and exhibit cross chess twinning (Figures 4A and 4C). Allanite is a notable accessory mineral, with metamict crystals that often fracture adjacent minerals (Figure 4B). Myrmekitic texture is common in all lithotypes (Figure 4D), which also display filigree and/or ribbon-type perthites.

Quartz-monzodiorite exhibit higher plagioclase content relative to alkalis and a gradual decrease in grain size, highlighting the size of plagioclase crystals relative to the matrix (Figures 4E, 4F, and 4G). These lithotypes show the most pronounced magma mixing textures, such as plagioclase crystals displaying synneusis texture (Figure 4H), zoning (Figures 4I and 4J), and corroded, rounded edges with box-cellular texture (Figures 4K and 4L). Additionally, they feature biotite blade textures (Figure 4M), mafic clots (Figure 4N), a mix of acicular and prismatic apatite (Figures 4O and 4P), and poikilitic textures. Some features related to magma mixing are observed in samples of syenogranite, monzogranite, granodiorite, and tonalite, such as plagioclase crystal zoning and poikilitic texture and box-cellular texture.

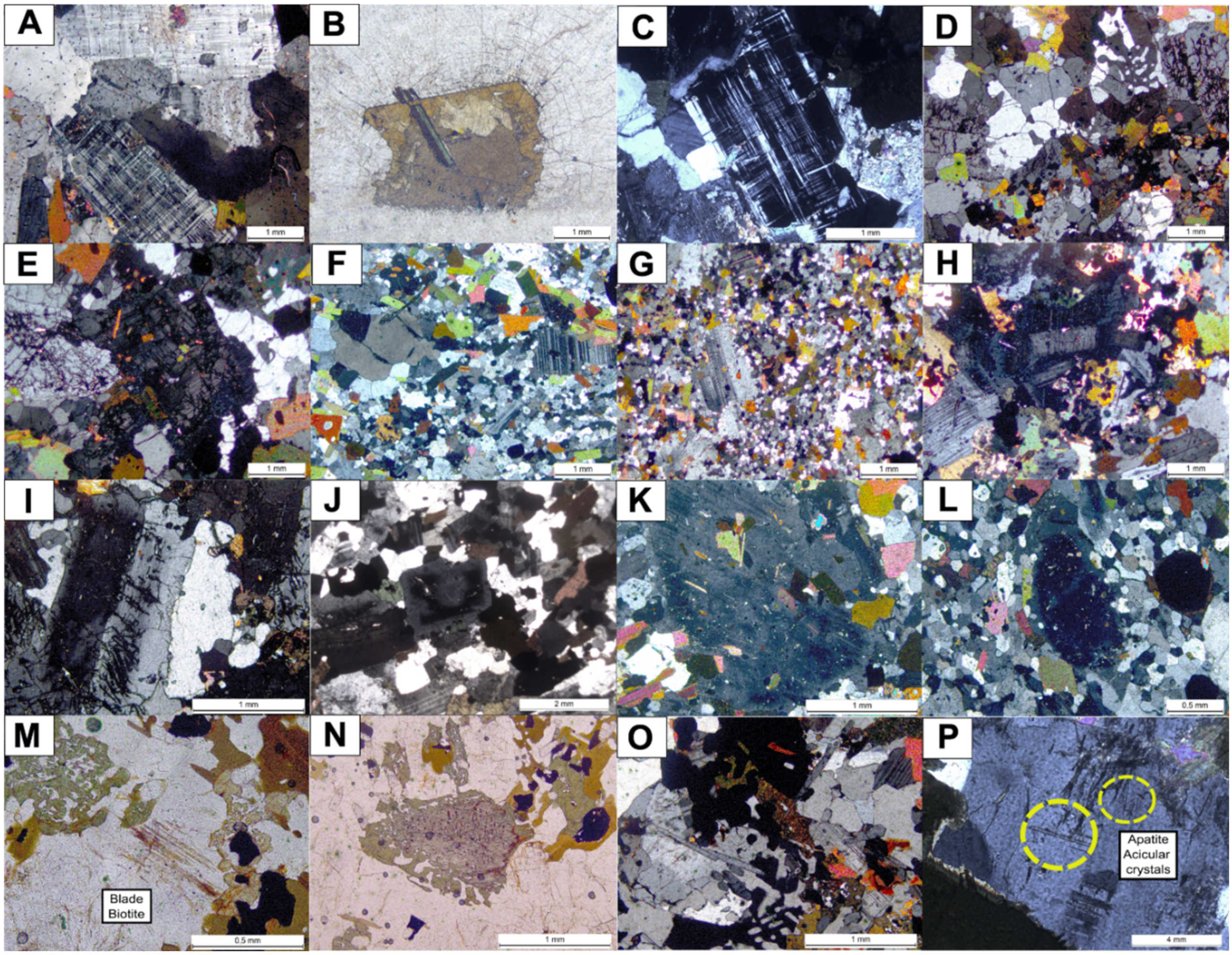

Figure 4 A. Microcline crystals displaying cross chess twinning in syenogranite; B. Metamict allanite fracturing a microcline crystal; C. Microcline crystal with cross chess twinning in monzogranite; D. Myrmekitic texture in syenogranite; E, F, and G. Larger plagioclase crystals in quartz-diorite lithotypes; H, I, and J. Zoned plagioclase crystals; K-L. Plagioclase crystals with corroded edges and box-cellular texture; M. Biotite blade with anomalous brown color; N. Mafic mineral clot with amphibole corona surrounding orthopyroxene; O-P. Mix of apatite crystals (acicular and prismatic).

4.2 Lithogeochemistry

Eighteen samples were selected for lithogeochemical analysis (major and trace elements), representing the mapped units within the PAIC: ocellar granite, monzogranite, syenogranite, granodiorite, tonalite and quartz-monzodiorite. The analytical results are presented in Supplementary Material 2. Geochemical data are grouped into three categories based on the mapped units: Group A – granite rocks; Group B – intermediary rocks; and Group C – ocellar granite.

The total variation in silica content is 20% (52.4–72.4 wt%) (Figure 5). The silica content in the granite rocks group ranges from 60.9.4 to 72.4 wt%, while ocellar granite exhibits silica values between 61.8 and 64.7 wt%. In intermediary rocks, silica content varies from 52.4 to 56.8 wt%. For MgO, MnO, Fe_2O_3, TiO_2, CaO, and P_2O_5, a similar trend of relative depletion is observed with increasing silica content (Figure 5).

Al_2O_3 shows enrichment in ocellar granite and in quartz-monzodiorite and shows relatively constant values in granite rocks (Figure 5). Na_2O shows a significant depletion in ocellar granites, and a slight relative enrichment in granite and intermediary rocks (Figure 5). Finally, K_2O exhibits strong enrichment in ocellar granite, and slight enrichment in the granite and intermediary groups (Figure 5).

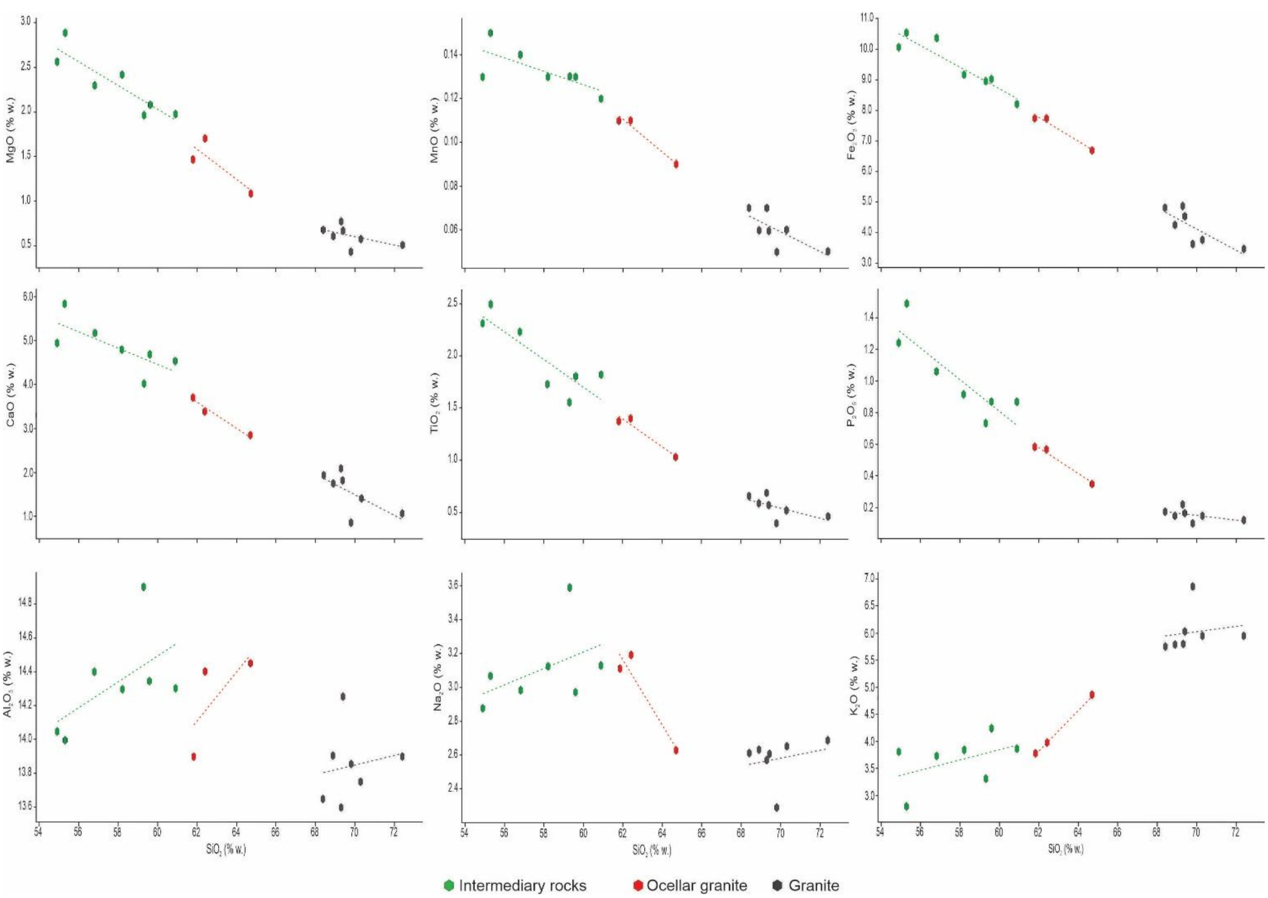

Figure 5 Binary diagrams from PAIC rocks (major elements versus silica). The Harker diagrams illustrate the evolutionary trend lines for the three distinct groups.

The MALI index [Na2O + K2O – CaO (wt%)] demonstrates the predominantly alkali-calcic trend of PAIC rocks (Figure 6), with only two samples, one granodiorite and one monzogranite/syenogranite, plotting in the alkaline field. The iron enrichment index [FeOt/(FeOt + MgO)] indicates that all rocks are ferroan (Figure 6). In contrast to the previous indices, the alumina saturation index (ASI) reveals differences among the rock groups: intermediary groups are essentially metaluminous, ocellar granites lie at the transition between the metaluminous and peraluminous fields, and granite samples are predominantly peraluminous (Figure 6). Finally, all samples are silica-saturated (Figure 6).

Chondrite-normalized Rare Earth Element (REE) patterns exhibit enrichment in Light Rare Earth Elements (LREE) relative to Heavy Rare Earth Elements (HREE) (LaN/YbN = 132.12–15.66) and negative Eu anomalies (Eu/Eu* = 0.78–0.32) for all samples, with more pronounced anomalies in the granite group (Figure 7). Two distinct patterns of LREE enrichment relative to HREE are observed within the granite group: three samples show stronger enrichment (LaN/YbN = 132.12–74), while the others exhibit patterns similar to the other two sample groups (LaN/YbN = 49.62–15.79) (Figure 7).

Principal Component Analysis (PCA) (Figure 8) reinforces the existence of three groups: a) granite group – These samples stand out in PCA due to strong influence on Principal Component 1 (PC1), linked to SiO2, K2O, and Rb. A subdivision within this group highlights samples PAIL 32, PAIL 37, and PAIL 46, which exhibit higher LREE enrichment (Figure 7) and strong influence from K2O (Figure 8); b) Intermediary rocks – Influenced by both Principal Components (PC1 and PC2). Notable exceptions include sample PAIL 25, with anomalously high Al2O3 and Zr concentrations, and sample PAIL 20, with high Zr concentration, both of which behave distinctly from other samples in this group (Figure 9); c) Ocellar granite – Primarily influenced by Principal Component 2 (PC2), associated with Al2O3 and Na2O oxides, as well as trace elements Zr, Nb, Ga, and Y (Figure 9).

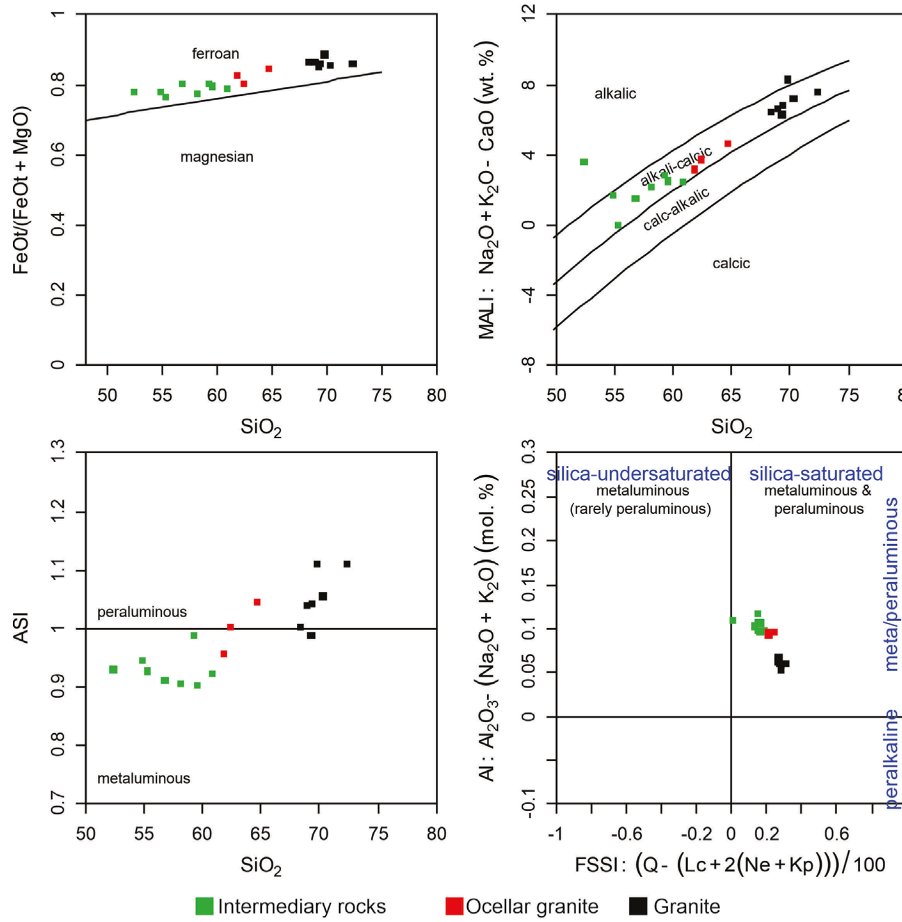

Figure 6 Classification diagrams for granitic rocks, adapted from Frost *et al.* (2001) and Frost & Frost (2008).

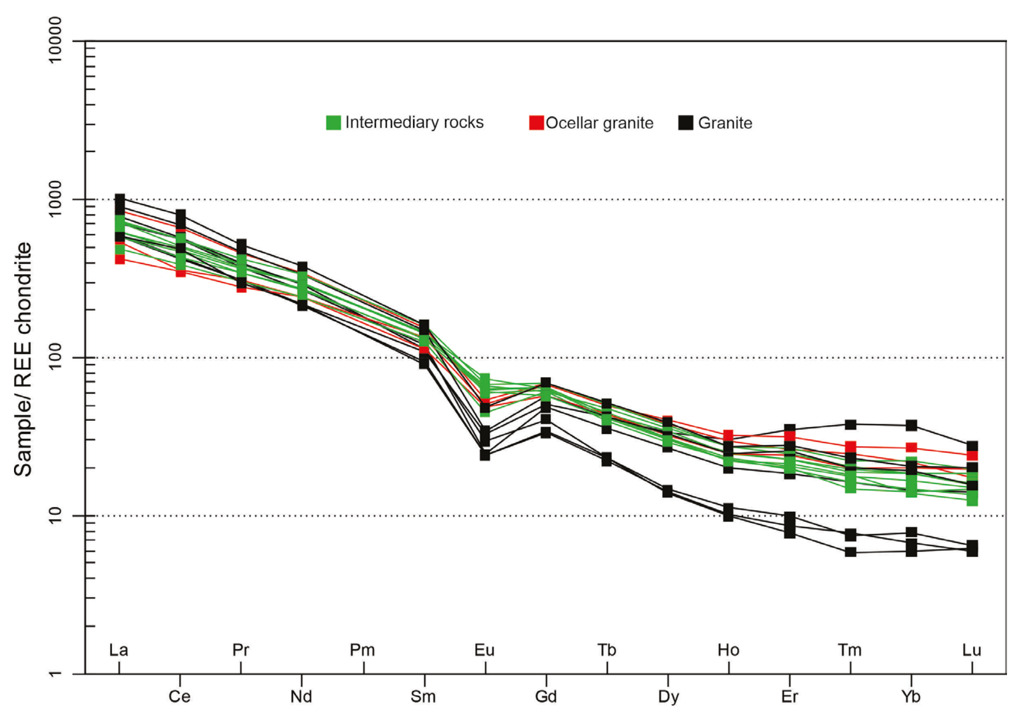

Figure 7 Multielement diagrams of the PAIC normalized for chondrite (Boynton 1984).

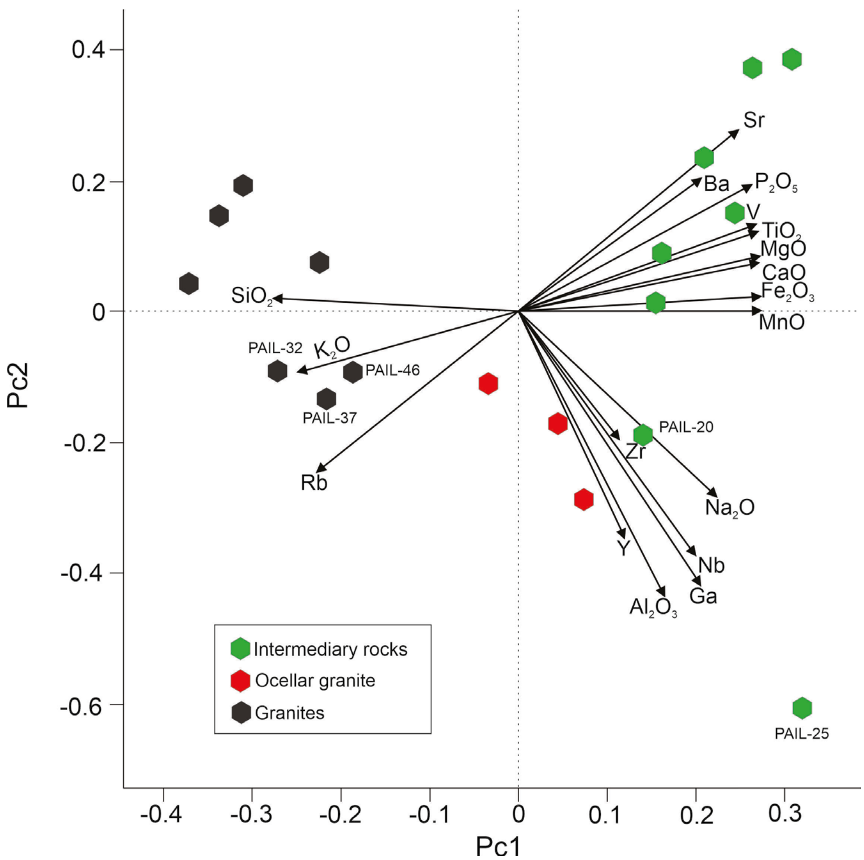

Figure 8 Biplot diagram (Principal Component Analysis) for oxides and trace elements, where the distance between the samples represents their similarity—closer points indicate greater similarity. The orientation of the vectors shows the relationship of each variable with the components. Variables with vectors pointing in similar directions indicate a positive correlation while opposing vectors indicate a negative correlation.

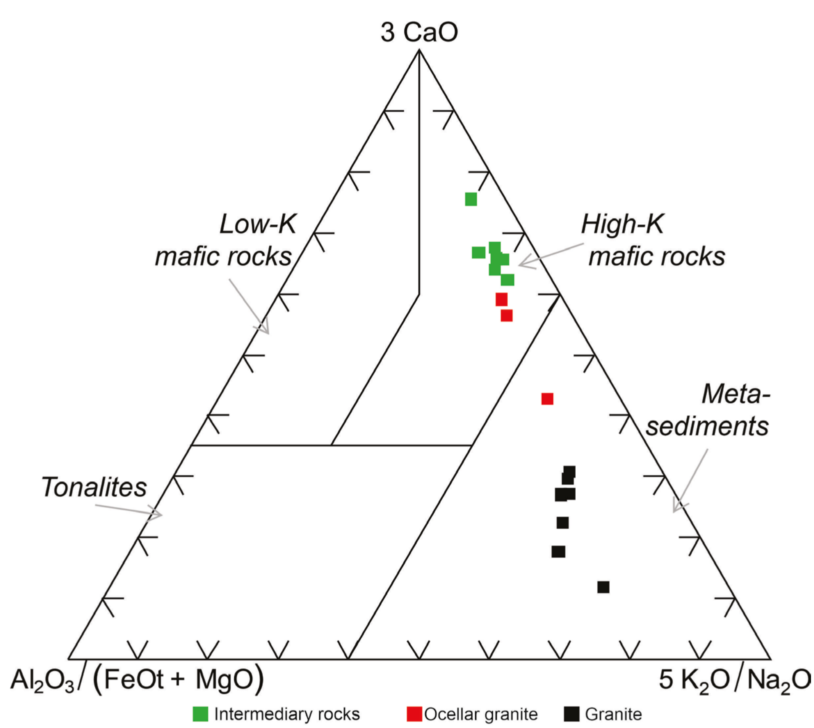

Figure 9 Discrimination diagrams of magmatic sources, adapted from Laurent *et al.* (2014).

The ternary diagram for granitoid magmatic sources, as proposed by Laurent *et al.* (2014), delineates two distinct fields for the PAIC samples (Figure 9). Granites plot within the field for magmas derived from metasedimentary rocks, along with one ocellar granite sample. Conversely, two ocellar granite samples and all intermediary samples plot within the field for magmas derived from high-K mafic rocks.

Figure 10 presents the results of binary mixing tests for rare earth elements (REE). Different models were evaluated to verify whether binary mixing between granite and quartz-monzodiorite samples could account for the composition of ocellar granites. For the test, the average composition of ocellar granite samples was calculated, and the endmembers were tested individually. The average REE composition of the ocellar granites can be explained by a mixture of approximately 65% of a quartz-monzodiorite magma (sample PAIL 20) and 35% of a granitic magma (sample PAIL 40A) (Figure 10).

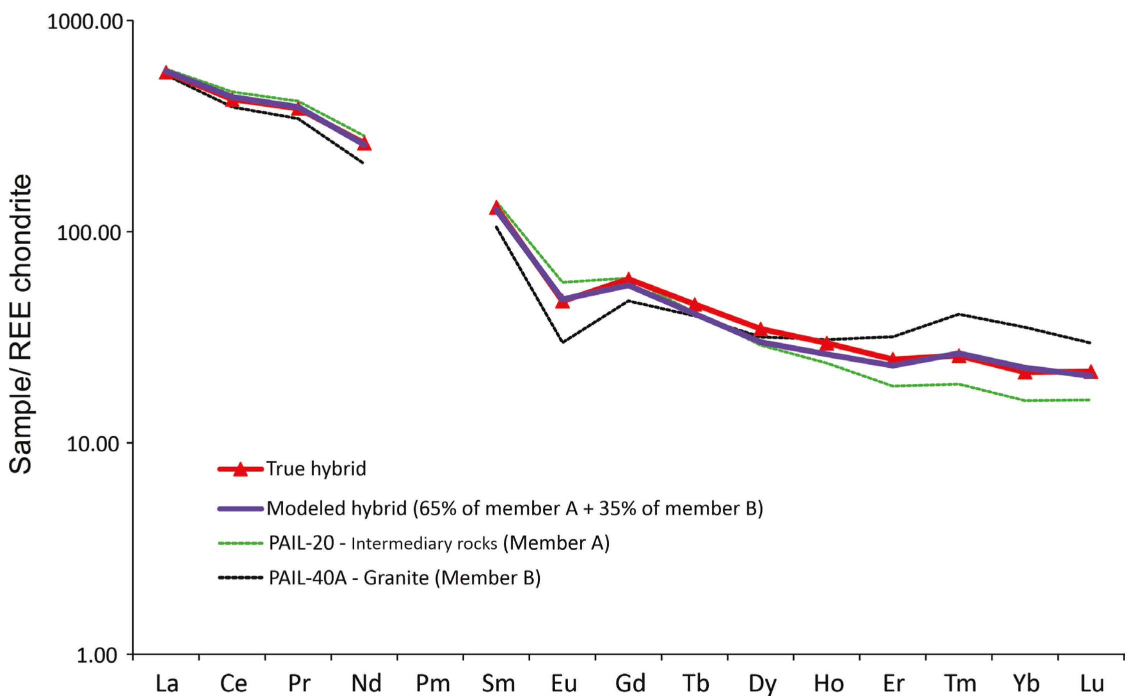

Figure 10 Diagram of the magma mixing modeling process between a granitic endmember (PAIL 40A) and a quartz-monzodiorite endmember, forming ocellar granite.

4.3 U-Pb geochronology

The analytical results for U-Pb zircon geochronology are presented in Supplementary Material 2, and cathodoluminescence images of the analyzed zircon grains are shown in Supplementary Material 3. Sample PAIL 01, classified as monzogranite, was collected within the Pedra Azul State Park. The zircon grains are predominantly euhedral, with some subhedral grains, prismatic pyramidal to bipyramidal shapes, and rounded terminations. They exhibit fractures and inclusions. Additionally, oscillatory zoning, typical of magmatic rocks, was observed, and there is evidence of more than one growth phase due to distinct core/rim patterns marked by luminescence differences. Sample PAIL 01 yielded a crystallization age of 501 ± 5 Ma, MSWD = 0.57, and a probability of 0.45 (N = 6) (Figure 11).

Zircon grains from sample PAIL 33A, classified as granodiorite, range from euhedral to anhedral, including short and long prismatic grains and grains with granular habits. Fractures and inclusions are common, as nebulitic textures and corroded rims, while oscillatory zoning is rare. Sample PAIL 33A yielded a crystallization age of 494 ± 4 Ma, MSWD = 0.35, and a probability of 0.56 (N = 22) (Figure 11).

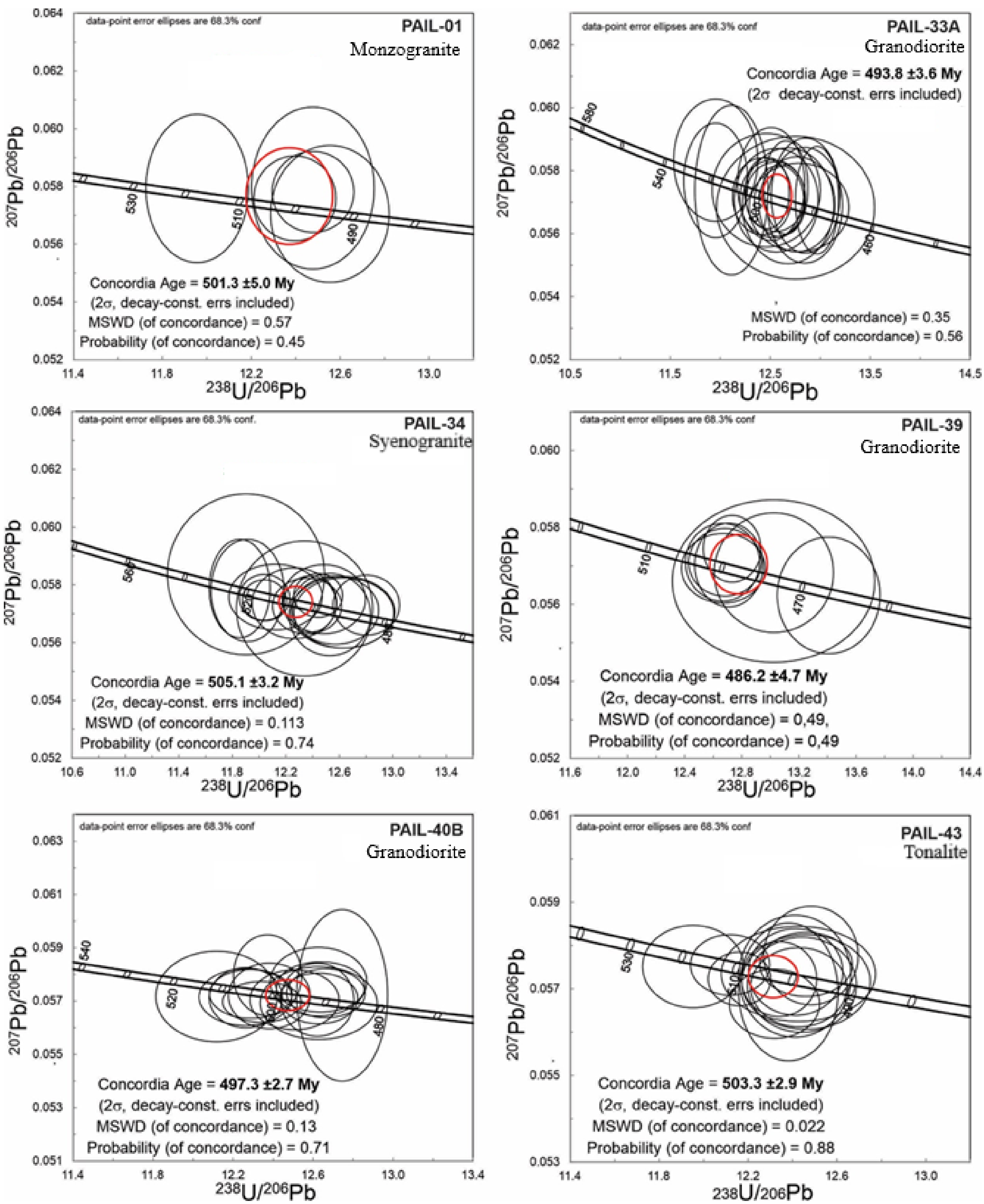

Figure 11 Concordia diagrams plotted as Tera-Wasserburg for the samples analyzed from the Pedra Azul Intrusive Complex. All ages were calculated at a 2-sigma confidence interval.

Sample PAIL 34, classified as syenogranite, contains mostly euhedral zircon grains, with a few subhedral examples. The grains are prismatic, with both elongated and short forms, while rounded grains are rare. Terminations range from pyramidal to bipyramidal, with fractures and inclusions present. Oscillatory zoning is the main characteristic. Sample PAIL 34 yielded a crystallization age of 505 ± 3 Ma, MSWD = 0.113, and a probability of 0.71 (N = 18) (Figure 11).

Sample PAIL 39, classified as granodiorite, exhibits euhedral to subhedral zircon grains, with short prismatic to rounded forms and pyramidal terminations. Fractures, inclusions, and oscillatory zoning are present. Sample PAIL 39 yielded a crystallization age of 486 ± 5 Ma, MSWD = 0.49, and a probability of 0.49 (N = 8) (Figure 11).

Zircon grains from sample PAIL 40B, classified as granodiorite, range from euhedral to anhedral, with a few grains displaying pyramidal terminations. Fractures and inclusions are present, oscillatory zoning is observed in a few grains, and nebulitic textures and corroded rims are common. Sample PAIL 40B yielded a crystallization age of 497 ± 3 Ma, MSWD = 0.13, and a probability of 0.71 (N = 17) (Figure 11).

Zircon grains from sample PAIL 43, classified as tonalite, range from euhedral to anhedral, with a few grains exhibiting pyramidal terminations. Oscillatory zoning is rarely observed, while nebulitic textures and corroded rims are common, alongside fractures and inclusions. Sample PAIL 43 yielded a crystallization age of 503 ± 3 Ma, MSWD = 0.022, and a probability of 0.88 (N = 17) (Figure 11).

5 Discussions

Post-collisional plutons of the Araçuaí Orogen in the southern region of Espírito Santo state exhibit compositions ranging from gabbro to granite and represent the last magmatic event observed in the orogen. These plutons display bimodal features, with bodies of tholeiitic compositions (*e.g.*, Jacutinga), medium- to high-K calc-alkaline compositions (*e.g.*, Santa Angélica, Alfredo Chaves, and Castelo), and alkaline compositions (*e.g.*, Venda Nova) (Aranda *et al.* 2020; Araujo *et al.* 2020; De Campos *et al.* 2004, 2016; Macêdo *et al.* 2022; Wiedemann *et al.* 2002). A notable feature of these intrusive complexes is the structural complexity and uniqueness, as well as field and petrographic evidence of magma mingling/mixing.

The PAIC is a post-collisional body of the Araçuaí Orogen composed of syenogranite, monzogranite, granodiorite, and quartz-monzodiorite. Unlike other post-collisional plutons in the region, which are inversely zoned (*e.g.*, granite margins and mafic cores in the Santa Angélica, Castelo, and Venda Nova intrusive complexes) (Araujo *et al.* 2020; Macêdo *et al.* 2022; Wiedemann *et al.* 2002), the PAIC features granitic margins and core, and the quartz monzodiorite occurs in isolated patches in the northern part of the massif. The complex is hosted by biotite-sillimanite gneiss to the west and quartzite to the east, rocks of the Nova Venécia Complex (Araujo *et al.* 2020, 2023; Gradim *et al.* 2014; Richter *et al.* 2016). At the PAIC margins, large roof-pendants of host rocks are observed, which are absent in the inner portions of the massif.

The PAIC exhibits features that reinforce evidence of magmatic coexistence. Structures such as mafic microgranular enclaves of varying compositions, sizes, and shapes (depending on composition, exhibiting a "salt- and-pepper" texture), net-veined granitic intrusions in quartz-monzodiorite - and quartz-monzodiorite -dominated areas, and pillow-like features where granitic intrusions isolate the quartz-monzodiorite host rocks have been observed. Additional features include chilled margins, ocellar zones, and hybridization zones at lithotype contacts. These observations are corroborated by petrographic evidence (Hibbard 1995), including zoned plagioclase crystals, boxy cellular textures, plagioclase crystals with corroded rims, mafic clots, poikilitic textures, a mix of acicular and prismatic apatite crystals, and biotite blade textures.

Geochemical data identified three groups corresponding to the mapped units within the PAIC: granite group, intermediary group and ocellar granite. Silica contents range from 52.4 to 72.4 wt%. The monzogranite/syenogranite group and ocellar granite occur at the margins of the PAIC, intruding metasedimentary rocks frequently observed as xenoliths and roof-pendants within the marginal granites. The high values of light rare earth elements (LREE) observed in these groups further support the possibility of crustal assimilation, as the rocks of the Nova Venécia Complex are characterized by high LREE, alkali, Al2O3, FeOt, and MgO contents (Araujo *et al.* 2013; Gradim *et al.* 2014; Richter *et al.* 2016). Conversely, the intermediary group, when plotted on the ternary diagram for magmatic sources (Laurent *et al.* 2014), falls within the high-K mafic rock field and may be associated with mafic granulitic rocks of the Juiz de Fora Complex or the Caparaó Complex (Faria *et al.* 2022; Mauri *et al.* 2024).

Globally, several granitic plutons are recognized for their bimodality, such as the Rastenberg Pluton in Austria (Gerdes, Worner & Finger 2000), the Jacaré Batholith in the Borborema Province (Sousa *et al.* 2022), and the Yamatu Pluton in China (Zhang *et al.* 2016).

Consistent with genetic proposals from literature data on post- tectonic magmatism processes and sources, geochemical magma mixing modeling reinforces field and petrographic evidence observed in the PAIC. It demonstrates that the composition of ocellar granites can be explained by the mixing of approximately 65% of a quartz-monzodiorite magma (sample PAIL 20) and 35% of a granitic magma (sample PAIL 40A).

The U-Pb zircon ages obtained via LA-ICP-MS indicate that the Pedra Azul Intrusive Complex crystallized between 505 and 485 Ma, consistent with post-collisional magmatism in the Araçuaí Orogen (De Campos *et al.* 2004, 2016; Pedrosa-Soares *et al.* 2011). These dates, together with the LA-ICP-MS zircon age obtained by Araujo *et al.* (2020) for a biotite granite sample from the PAIC margin, with a crystallization age of 523 ± 2 Ma, are within the post-collisional context of the Araçuaí Orogen. The post-collisional magmatism of the Ribeira Belt is marked by two crystallization peaks: an older Cambrian peak that produced the Suruí Suite (ca. 510 Ma) and a younger Ordovician peak that generated the Nova Friburgo Suite (ca. 485 Ma) (Bione *et al.* 2019; Bongiolo *et al.* 2016; Schmitt *et al.* 2004; Valeriano *et al.* 2011, 2016). Araujo *et al.* (2020) propose two crystallization peaks for post-collisional plutons in the Araçuaí Orogen: one between 530–515 Ma and another between 505–490 Ma.

The granite sample dated by Araujo *et al.* (2020) corresponds to the older peak, similar to other post-collisional plutons in the region. These include LA-ICP-MS zircon ages of 524 ± 5 Ma and 522 ± 13 Ma for monzogranite samples from the Castelo Intrusive Complex (Macêdo *et al.* 2022), 515 ± 3 Ma for monzogranite from the Santa Angélica Intrusive Complex (Potratz *et al.* 2022), 527 ± 2 Ma for tonalite from the Mestre Álvaro Massif (Araujo *et al.* 2022), 531 ± 4 Ma for syenogranite from the Alto Chapéu Intrusive Complex (Teixeira *et al.* 2020), 531 ± 34 Ma for granite from the Pedra do Elefante Massif (De Campos *et al.* 2016), and 524 ± 7 Ma for norite from the São Gabriel Baunilha Massif (Wisniowski *et al.* 2021).

The PAIC samples dated range from 505 to 485 Ma, corresponding to the younger magmatic peak in the Araçuaí Orogen. These dates align with ages obtained for the Castelo Intrusive Complex, such as 486 ± 6 Ma for quartz- monzodiorite and 499 ± 4 Ma for monzogranite (Macêdo *et al.* 2022), as well as 481 ± 3 Ma and 496 ± 3 Ma for quartz-monzonite and monzogabbro, respectively, from the Afonso Cláudio Intrusive Complex (Aranda *et al.* 2020). Additionally, ages of 488 ± 7 Ma for charnockite in the Pedra do Elefante Massif (De Campos *et al.* 2016) and 496 ± 2 Ma and 501 ± 4 Ma for syenomonozonite and gabbro in the Venda Nova Intrusive Complex (Bellon *et al.* 2022) are consistent with this younger peak.

Bione *et al.* (2019) propose for the Ribeira Belt that a broader distribution of crystallization peaks (ca. 515, 495, and 455 Ma) may be attributed to analytical errors or that a single continuous event occurred between 515 and 475 Ma. For the Araçuaí Orogen, Potratz *et al.* (2022) suggest three peaks for rocks in the Santa Angélica Intrusive Complex: an older peak at 537 ± 5 Ma, marking the transition from syn-collisional to post-collisional stages; an intermediate peak at 510 ± 5 Ma, representing the climax of post-collisional magmatism; and a younger peak at 488 ± 7 Ma, marking the end of post-collisional magmatic activity. Macêdo *et al.* (2022) also report magmatic activity around 426 ± 15 Ma in leucocratic dikes within the Castelo Intrusive Complex.

Although debates on crystallization peaks for post-collisional magmatism in the Araçuaí Orogen are ongoing, the ages obtained for various lithotypes across different plutons indicate intense magmatic activity lasting at least 50 million years. The orogenic collapse of the Araçuaí Orogen caused decompression and melting of the lower crust and asthenospheric mantle, which ascended through deep faults to form these plutons (De Campos *et al.* 2016; Serrano *et al.* 2018). However, unlike other post-collisional plutons, mantle participation in the PAIC appears to be less pronounced, as suggested by geochemical data, indicating that mantle-derived magma primarily acted as a heat source, inducing crustal melting and mixing.

6 Conclusions

The Pedra Azul Intrusive Complex (PAIC) illustrates the complexity seen in many post-collisional plutons of the Araçuaí Orogen. Petrographic and geochemical evidence demonstrates compositional diversity and the co-genetic relationship among these magmas. Field and petrographic evidence supports mixing features, including mafic microgranular enclaves, pillow-like structures, chilled margins, ocelli, and zoned plagioclase crystals with boxy cellular textures, corroded rims, and biotite blades.

Geochemical data suggest different sources for PAIC rocks, including nearby units such as the Nova Venécia Complex and mafic orthogneisses from the Juiz de Fora and Caparaó Complexes. Mixing models demonstrated that the ocellar granite's composition could result from a mixture of two end-members, confirming the co-genetic relationship among these rocks and the complex interplay of magmatic processes in the Araçuaí Orogen.

Finally, U-Pb zircon geochronology data are consistent with the post-collisional stage of the orogen, showing that this phase was marked by intense magmatic activity, with the PAIC's magmatism lasting at least 20 million years.

7 Supplementary material

The following online material is available for this article:

Supplementary Material 1: QAPF Diagram and Modal Composition.
Supplementary Material 2: Lithogeochemical Table of the PAIC.
Supplementary Material 3: Cathodoluminescence Images of Paic Zircon Grains.

8 Acknowledgments

The authors thank the funding agencies. Guilherme Loriato Potratz thanks Fundação Carlos Chagas Filho de Amparo à Pesquisa do Estado do Rio de Janeiro for his post doctoral scholarship, process numbers E26-204.530/2021 and E26-204.531/2021. Mauro Cesar Geraldes thanks the National Council for Scientific and Technological Development (CNPq) for the research grant (process nº 301470/2016-2).

9 References

Alkmim, F.F., Marshak, S., Pedrosa-Soares, A.C., Peres, G.G., Cruz, S.C.P. & Whittington, A. 2006, 'Kinematic evolution of the Araçuaí-West Congo orogen in Brazil and Africa: Nutcracker tectonics during the Neoproterozoic assembly of Gondwana', *Precambrian Research*, vol. 149, pp. 43–64, DOI:10.1016/j.precamres.2006.06.007

Alkmim, F.F., Pedrosa-soares, A.C., Noce, C.M., Cerqueira, S. & Cruz, P. 2007, 'Sobre a Evolução Tectônica do Orógeno Araçuaí-Congo Ocidental', *Geonomos*, vol. 15, pp. 25–43, DOI:10.18285/geonomos.v15i1.105

Alkimim, F.F., Kuchenbecker, M., Reis, H.L.S. & Pedrosa-Soares, A.C. 2017, 'The Araçuaí belt', in M. Heilbron, U.G. Cordani, F.F. Alkmim (eds), *São Francisco Craton, Eastern Brazil*, Regional Geology Reviews, Springer International Publishing Co, pp. 255–276.

Amaral, L., Caxito, F.A., Pedrosa-Soares, A.C., Queiroga, G., Babinski, M., Trindade, R., Lana, C. & Chemale, F. 2020, 'The Ribeirão da Folha ophiolite-bearing accretionary wedge (Araçuaí orogen, SE Brazil): new data for Cryogenian plagiogranite and metasedimentary rocks', *Precambrian Research*, 336, 105522, DOI:10.1016/j.precamres.2019.105522

Araujo, C., Pedrosa-Soares, A., Lana, C., Dussin, I., Queiroga, G., Serrano, P. & Medeiros- Júnior, E. 2020, 'Zircon in emplacement borders of post-collisional plutons compared to country rocks: a study on morphology, internal texture, U–Th–Pb geochronology and Hf isotopes (Araçuaí orogen, SE Brazil)', *Lithos*, vol. 352–353, pp. 1–18, DOI:10.1016/j.lithos.2019.105252

Araujo, C., Pedrosa-Soares, A., Lana, C., Tedeschi, M., Roncato, J., Dussin, I., Serrano, P. & Dantas, E. 2023, 'Tracking a magmatic arc within a confined orogen: new evidence from the Araçuaí orogen (SE Brazil)', *Journal of South American Earth Science*, vol. 129, pp. 1–22, DOI:10.1016/j.jsames.2023.104490

Aranda, R.O., Chaves, A.O., Medeiros Júnior, E.B. & Venturini Junior, R. 2020, 'Petrology of the Afonso Cláudio Intrusive Complex: new insights for the Cambro-Ordovician post-collisional magmatism in the Araçuaí-West Congo orogen, southeast Brazil', *Journal of South American Earth Science*, vol. 98, pp. 1–19, DOI:10.1016/j.jsames.2019.102465

Babinski, M., Pedrosa-Soares, A.C., Trindade, R.I.F., Martins, M., Noce, C.M. & Liu, D. 2012, 'Neoproterozoic glacial deposits from the Araçuaí Orogen, Brazil: Age, provenance and correlations with the São Francisco craton and West Congo belt', *Gondwana Research*, vol. 21, pp. 451-465, DOI:10.1016/j.gr.2011.04.008

Bellon, U.D., Souza Junior, G.F., Temporim, F.A., D'Agrella-Filho, M.S. & Trindade, R.I.F. 2022, 'U-Pb geochronology of a reversely zoned pluton: records of pre-to-post collisional magmatism of the Araçuaí belt (SE- Brazil)?', *Journal of South American Earth Science*, 119, pp. 1–15, DOI:10.1016/j.jsames.2022.104045

Bione, F.R.A., Bongiolo, E.M., Mendes, J.C. & Roland, C.L. 2019, 'Geochemistry, Sm-Nd isotopes and SHRIMP U-Pb geochronology of the Morro do Coco Granite (RJ, Brazil): Another piece of the post-collisional magmatism of the Ribeira Belt. Braz', *Journal of Geology*, vol. 49, pp. 1–19, DOI:10.1590/2317-4889201920190010

Bongiolo, E.M., Renac, C., Piza, P.D.A.T., Schmitt, R.S. & Mexias, A.S. 2016, 'Origin of pegmatites and fluids at Ponta Negra (RJ, Brazil) during late- to post-collisional stages of the Gondwana Assembly', *Lithos*, vol. 240–243, pp. 259–275, DOI:10.1016/j.lithos.2015.11.015

Bonin, B. 2004, 'Do coeval mafic and felsic magmas in post-collisional to within-plate regimes necessarily. imply two contrasting, mantle and crustal, sources? A review'. *Lithos*, 78, pp. 1 24, DOI:10.1016/j.lithos.2004.04.042

Boynton, W.V. 1984, 'Cosmochemistry of the rare earth elements: meteoritic studies', in P. Hendersen (ed), *Rare Earth Elements Geochemistry*, Elsevier, Amsterdam, pp. 63–114.

Caxito, F.A., Hartmann, L.A., Heilbron, M., Pedrosa-Soares, A.C., Bruno, H., Basei, M.A. & Chemale, F. 2022, 'Multi-proxy evidence for subduction of the Neoproterozoic Adamastor Ocean and Wilson cycle tectonics in the South Atlantic Brasiliano Orogenic System of Western Gondwana', *Precambrian Research*, vol. 376, 106678, DOI:10.1016/j.precamres.2022.106678

Costa-de-Moura, J., Wiedemann, C.M., Nascimento R.C.C., Vriend S. & Silva, D.B.M. 1997, 'Geologia, petrografia e geoquímica do Complexo Intrusivo de Pedra Azul, Espírito Santo', Proceedings of Academia Brasileira de Ciências, vol. 69, no. 1.

De Campos, C.P., Cezar Mendes, J., Ludka, I.P., Medeiros, S.R., Moura, J.C. & Wallfass, C. M. 2004, 'A review of the Brasiliano magmatism in southern Espírito Santo, Brazil, with emphasis on post-collisional magmatism', *Journal of Virtual Explorer*, vol. 17, pp. 1–39, DOI:10.3809/jvirtex.2004.00106

De Campos, C.P., Medeiros, S.R., Mendes, J.C., Pedrosa-Soares, A.C., Dussin, I., Ludka, I. P. & Dantas, E.L. 2016, 'Cambro-ordovician magmatism in the Araçuaí belt (SE Brazil): snapshots from a post-collisional event', *Journal of South American Earth Science*, vol. 68, pp. 248–268, DOI:10.1016/j.jsames.2015.11.016

Degler, R., Pedrosa-Soares, A., Novo, T., Tedeschi, M., Silva, L.C., Dussin, I. & Lana, C. 2018, 'Rhyacian-Orosirian isotopic records from the basement of the Araçuaí-Ribeira orogenic system (SE Brazil): links in the Congo-São Francisco palaeocontinent', *Precambrian Research*, vol. 317, pp. 179–195, DOI:10.1016/j.precamres.2018.08.018

Dewey, J.F. 1988, 'Extensional collapse of orogens', *Tectonics*, vol. 7, pp. 1123-1139.

Faria, T.G., Alves, M.I., Potratz, G.L., Silva, L.F.R., Rodrigues, S.W.O., Martins, M.V.A. & Geraldes, M.C. 2022, 'The Serra do Caparaó Complex, Mantiqueira Province, Brazil, revisited: Metamorphic age constraints by U-Pb and Lu-Hf method in zircon by LA-ICPMS', *Journal of Geological Survey of Brazil*, vol. 5, pp. 49–80, DOI:10.29396/jgsb.2022.v5.n1.1

Frost, B.R. & Frost, C.D. 2008, 'A geochemical classification for feldspathic igneous rocks', *Journal of Petrology*, vol. 49, pp. 1955–1969,DOI:10.1093/petrology/egn054

Frost, B.R., Arculus, R.J., Barnes, C.G., Collins, W.J., Ellis, D.J. & Frost, D.C. 2001, 'A geochemical classification of granitic rocks', *Journal of Petrology*, vol. 42, pp. 2033–2048, DOI:10.1093/petrology/42.11.2033

Gerdes, A., Worner, G. & Finger, F. 2000, 'Hybrids, magma mixing and enriched mantle melts in post-collisional Variscan granitoids: the Rastenberg Pluton, Austria', in W. Franke, V. Haak, O. Oncken, D. Tanner (eds), Orogenic Processes: Quantification and Modelling in the Variscan Belt, *Geological Society*, London, Special Publications, vol. 179, pp. 415-431, DOI:10.1144/GSL.SP.2000.179.01.25

Gómez-Frutos, D., Castro, A. & Gutiérrez-Alonso, G. 2023, 'Post-collisional batholiths do contribute to continental growth', *Earth and Planetary Science Letters*, vol. 603, 117978, DOI:10.1016/j.epsl.2022.117978

Gonçalves, L., Farina, F., Lana, C., Pedrosa-Soares, A.C., Alkmim, F. & Nalini, H.A. 2014, 'New U-Pb ages and lithochemical attributes of the Ediacaran Rio Doce magmatic arc, Araçuaí confined orogen, southeastern Brazil', *Journal of South American Earth Science*, 52, 129–148, DOI:10.1016/j.jsames.2014.02.008

Gonçalves, L., Alkmim, F.F., Pedrosa-Soares, A.C., Dussin, I.A., Valeriano, C.M., Lana, C. & Tedeschi, M. 2016, 'Granites of the intracontinental termination of a magmatic arc: an example from the Ediacaran Araçuaí orogen, southeastern Brazil', *Gondwana Research*, vol. 36, pp. 439–458, DOI:10.1016/j.gr.2015.07.015

Gonçalves, L., Alkmim, F.F., Pedrosa-Soares, A., Gonçalves, C.C.& Vieira, V. 2018, 'From the plutonic root to the volcanic roof of a continental magmatic arc: a review of the Neoproterozoic Araçuaí orogen, southeastern Brazil', *International Journal Earth Science*, vol. 107, pp. 337–358, DOI:10.1007/s00531-017-1494-5

Gouvêa, L.P., Medeiros, S.R., Mendes, J.C., Soares, C., Marques, R. & Melo, M. 2020, 'Magmatic activity period and estimation of P-T metamorphic conditions of Pre- Collisional Opx-Metatonalite from Araçuaí-Ribeira orogens boundary, SE Brazil', *Journal of South American Earth Science*, vol. 99, 102506, DOI:10.1016/j.jsames.2020.102506

Gradim, C., Roncato, J., Pedrosa-Soares, A.P., Cordani, U., Dussin, I., Alkmim, F.F., Queiroga, G., Jacobsohn, T., Silva, L.C. & Babinski, 2014, 'The hot back-arc zone of the Araçuaí orogen, Eastern Brazil: from sedimentation to granite generation', *Brazilian Journal of Geology*, vol. 44, pp. 155–180, DOI:10.5327/Z2317-48892014000100012

Harker, A. 1956, *Petrology for Students. An Introduction to the Study of Rocks under the Microscope*, 8a ed. Cambridge University Press, Cambridge.

Harris, N. B. W., Pearce, J. A. & Tindle, A.G. 1986, 'Geochemical characteristics of collision zone magmatism', in M.P. Coward & A.C. Ries (eds), *Collision Tectonics*, Geological Society, London, Special Publications 19, pp. 67- 82.

Heilbron, M.L., Pedrosa-Soares, A.C., Campos Neto, M.C., Silva, L.C., Trouw, R. & Janasi, V.A. 2004, 'Brasiliano Orogens in Southeast and South Brazil', *Journal of Virtual Explorer*, vol. 17, paper 4, DOI:10.3809/jvirtex.2004.00109

Hibbard, M.J. 1995, *Petrography to Petrogenesis*, Prentice Hall, Englewood Cliffs, New Jersey.

Jackson, S.E., Pearson, N.J. & Griffin, E.A. 2004, 'The application of laser ablation–inductively coupled plasma– mass spectrometry to *in situ* U–Pb zircon geochronology', *Chemical Geology*, pp. 47-69, DOI:10.1016/j.chemgeo.2004.06.017

Kuchenbecker, M., Pedrosa-Soares, A.C., Babinski, M., & Fanning, M. 2015, 'Detrital zircon age patterns and provenance assessment for pre-glacial to post-glacial successions of the Neoproterozoic Macaúbas Group, Araçuaí orogen, Brazil', *Precambrian Research*, vol. 266, pp. 12–26, DOI:10.1016/j.precamres.2015.04.016

Laurent, A., Janousek, V., Magna, T., Schulmann, K. & Miková, J. 2014, 'Petrogenesis and geochronology of a post-orogenic calc-alkaline magmatic association: the Žulová Pluton, Bohemian Massif', *Journal of Geoscience*, vol. 59, pp. 415–440, DOI:10.3190/jgeosci.176

Liégeois, J.P., Navez, J., Hertogen, J. & Black, R. 1998, 'Contrasting origin of post-collisional high-K calc-alkaline and shoshonitic versus alkaline and peralkaline granitoids: the use of sliding normalization', *Lithos*, vol. 41, pp. 1–28, DOI:10.1016/S0024-4937(98)00023-1

Ludka, I.P. & Wiedemann-Leonardos, C.M. 2000, 'Further signs of an enriched mantle source under the neoproterozoic Araçuaí-Ribeira mobile belt', *Revista Brasileira de Geociências*, vol. 30, pp. 95–98, DOI: 10.25249/0375-7536.2000301095098

Macêdo, I.M.L., Geraldes, M.C.G., Marques, R.A., Melo, M.G., Tavares, A.D., Martins, M.V.A., Oliveira, H.C. & Rodrigues, R.D. 2022, 'New clues for magma-mixing processes using petrological and geochronological evidence from the Castelo Intrusive Complex, Araçuaí Orogen (SE Brazil)', *Journal of South American Earth Science*, vol. 115, 103758, DOI:10.1016/j.jsames.2022.103758

Mauri, S., Heilbron, M., Bruno, H., Bersan, S., Almeida, R., Marques, R.A., Lacerda, S., Souza, A.M., Paravidini, G., Neto, C., Valeriano, C.M., Chapman, G., Fowler, M., Mottram, C., Strachan, R. & Storey, C. 2024, 'Coeval TTG and sanukitoid magmatism during the Rhyacian tectonic evolution of the Juiz de Fora Complex (São Francisco Paleocontinent, SE-Brazil)', *Precambrian Research*, vol. 414, 107585, DOI: 10.1016/j.precamres.2024.107585

Medeiros, S.R., Wiedeman-Leonardos, C.M. & Mendes, J.C. 2000, 'Post-collisional multistage magmatism in the Ribeira mobile belt; geochemical and isotopic study of the Varzea Alegre intrusive complex, Espírito Santo, Brazil', *Revista Brasileira de Geociências*, vol. 30, pp. 30–34, DOI:10.25249/0375-7536.2000301030034

Melo, M.G., Lana, C., Stevens, G., Pedrosa-Soares, A.C., Gerdes, A., Alkmin, L.A., Nalini, H.A. & Alkmim, F.F. 2017a, 'Assessing the isotopic evolution of S-type granites of the Carlos Chagas Batholith, SE Brazil: clues from U–Pb, Hf isotopes, Ti geothermometry and trace element composition of zircon', *Lithos*, vol. 284–285, pp. 730– 750, DOI:10.1016/j.lithos.2017.05.025

Melo, M.G., Stevens, G., Lana, C., Pedrosa-Soares, A.C., Frei, D., Alkmim, F.F. & Alkmin, L.A. 2017b, 'Two cryptic anatectic events within a syn-collisional granitoid from the Araçuaí orogen (southeastern Brazil): evidence from the polymetamorphic Carlos Chagas batholith', *Lithos*, vol. 277, pp. 51–71, DOI:10.1016/j.lithos.2016.10.012

Melo, M.G., Lana, C., Stevens, G., Hartwig, M.E. & Pimenta, M.S. 2020, 'Deciphering the source of multiple U- Pb ages and complex Hf isotope composition in zircon from post-collisional charnockite-granite associations from the Araçuaí Orogen (southeastern Brazil)', *Journal of South American Earth Science*, vol. 103, 102792, DOI:10.1016/j.jsames.2020.102792

Mendes, J.C. & De Campos, C.M.P. 2012, 'Norite and charnockites from the Venda Nova Pluton, SE Brazil: intensive parameters and some petrogenetic constraints', *Geoscience Frontiers*, vol. 3, pp. 789–800, DOI:10.1016/j.gsf.2012.05.009

Niu, Y., Zhao, Z., Zhu, D. C. & Mo, X. 2013, 'Continental collision zones are primary sites for net continental crust growth—attestable hypothesis', *Earth-Science Reviews*, vol. 127, pp. 96–110, DOI:10.1016/j.earscirev.2013.09.004

Noce, C.M., Pedrosa-Soares, A.C., Piuzana, D., Armstrong, R., Laux, J.H., Campos, C.M. & Medeiros, S.R. 2004, 'Ages of sedimentation of the kinzigitic complex and of alate orogenic thermal episode in the Araçuaí orogen Northern Espírito Santo State, Brazil: Zircon and monazite U–P SHRIMP and ID-TIMS data', *Revista Brasileira de Geociências*, vol. 34, pp. 587–592.

Pedrosa-Soares, A.C., Noce, C.M., Wiedemann, C.M. & Pinto, C.P. 2001, 'The Araçuaí- West-Congo Orogen in Brazil: an overview of a confined orogen formed during Gondwanaland assembly', *Precambrian Research*, vol. 110 (1–4), pp. 307–323, DOI:10.1016/S0301-9268(01)00174-7

Pedrosa-Soares, A.C., Noce, C.M., Alkmim, F.F., da Silva, L.C., Babinski, M., Cordani, U. & Castañeda, C. 2007, 'Orógeno Araçuaí: Síntese do conhecimento 30 anos após Almeida 1977', *Geonomos*, vol. 15, pp. 1–16, DOI:10.18285/geonomos.v15i1.103

Pedrosa-Soares, A.C., De Campos, C.P., Noce, C., Silva, L.C., Novo, T., Roncato, J., Medeiros, S., Castañeda, C., Queiroga, G., Dantas, E., Dussin, I. & Alkmim, F. 2011, 'Late Neoproterozoic – Cambrian Granitic Magmatism in the Araçuaí orogen (Brazil), the Eastern Brazilian Pegmatite Province and Related Mineral Resources', *Geological Society*, London, Special Publications, vol. 350, pp. 25–51, DOI:10.1144/SP350.3

Pedrosa-Soares, A.C., Deluca, C., Araujo, C., Gradim, C., Lana, C., Dussin, I., Silva, L.C. & Babinski, M. 2020, 'O Orógeno Araçuaí à luz da geocronologia: um tributo a Umberto Cordani', in A. Bartorelli, W. Teixeira, B.B. Brito Neves (eds), *Geocronologia e Evolução Tectônica do Continente Sul-Americano: a contribuição de Umberto Giuseppe Cordani*, Solarias Edições Culturais, São Paulo.

Potratz, G.L., Geraldes, M.C., Medeiros Júnior, E.B., Temporim, F.A. & Martins, M.V.A. 2022, 'A Juvenile Component in the Pre- and Post-Collisional Magmatism in the Transition Zone between the Araçuaí and Ribeira Orogens (SE Brazil)', *Minerals*, vol. 12, pp. 1–22, DOI:10.3390/min12111378

Queiroga, G.N., Pedrosa-Soares, A.C., Noce, C.M., Alkmim, F.F., Pimentel, M.M., Dantas, E.L., Martins, M., Castañeda, C., Suita, M.T.F. & Prichard, H. 2007, 'Age of the Ribeirão da Folha ophiolite, Araçuaí Orogen: the U-Pb zircon (LA-ICPMS) dating of a plagiogranite', *Geonomos*, vol. 15, no. 1, pp. 61–65, DOI:10.18285/geonomos. v15i1.107

Richter, F., Lana, C., Stevens, G., Buick, I., Pedrosa-Soares, A.C., Alkmim, F.F. & Cutts, K. 2016, 'Sedimentation, metamorphism and granite generation in a back-arc region: records from the Ediacaran nova Venécia Complex (Araçuaí orogen, southeastern Brazil)', *Precambrian Research*, vol. 272, pp. 78–100, DOI:10.1016/j.precamres.2015.10.012

Sami, M., Ntaflos, T., Farahat, E.S., Mohamed, H.A., Hauzenberger, C. & Ahmed, A.F. 2018, 'Petrogenesis and geodynamic implications of Ediacaran highly fractionated A-type granitoids in the north Arabian-Nubian Shield (Egypt): constraints from whole- rock geochemistry and Sr-Nd isotopes', *Lithos*, vol. 304–307, pp. 329–346, DOI:10.1016/j.lithos.2018.02.015

Santiago, R., Caxito, F.A., Pedrosa-Soares, A., Neves, M.A. & Dantas, E.L. 2020, 'Tonian island. Arc remnants in the northern Ribeira orogen of western Gondwana: the Caxixe batholith (Espírito Santo, SE Brazil)', *Precambrian Research*, vol. 351, DOI:10.1016/j.precamres.105944

Santiago, R., Caxito, F.A., Pedrosa-Soares, A., Neves, M.A., Calegari, S.S. & Lana, C. 2022, 'Detrital zircon U–Pb and Lu–Hf constraints on the age, provenance and tectonic setting of arc-related high-grade units of the transition zone of the Araçuaí and Ribeira orogens (SE Brazil)', *Journal of South American Earth Science*, vol. 116, 103861, DOI:10.1016/j.jsames.2022.103861

Santiago, R., Caxito, F.A., Pedrosa-Soares, A., Neves, M.A., Dantas, E.L., Calegari, S.S. & Lana, C. 2023, 'Records of the accretionary, collisional and post-collisional evolution of western Gondwana in the high-grade core of the Araçuaí-

Ribeira orogenic system, SE Brazil', *Precambrian Research*, vol. 397, 107191, DOI:10.1016/j.precamres.2023.107191

Schmitt, R.S., Trouw, R.A.J., Van Schmus, W.R. & Pimentel, M.M. 2004, 'Late amalgamation in the central part of West Gondwana: new geochronological data and the characterization of a Cambrian collisional orogeny in the Ribeira Belt (SE Brazil)', *Precambrian Research*, vol. 133, pp. 29–61, DOI:10.1016/j.precamres.2004.03.010

Sengor, A.M.C., Ozeren, M.S., Keskin, M., Sakinç, M., Ozbakir, A.D. & Kayan, I. 2008, 'Eastern Turkish high plateau as a small Turkic-type orogen: Implications for post-collisional crust-forming processes in Turkic-type orogens', *Earth-Science Reviews*, vol. 90, pp. 1-48, DOI:10.1016/j.earscirev.2008.05.002

Serrano, P., Pedrosa-Soares, A., Medeiros-Júnior, E., Fonte-Boa, T., Araujo, C., Dussin, I., Queiroga, G. & Lana, C. 2018, 'A-type Medina batholith and post-collisional anatexis in the Araçuaí orogen (SE Brazil)', *Lithos*, vol. 320– 321, pp. 515–536, DOI:10.1016/j.lithos.2018.09.009

Soares, C., Queiroga, G., Pedrosa-Soares, A., Gouvêa, L.P., Valeriano, C.M., de Melo, M. G. & Delicio, R. 2020, 'The Ediacaran Rio Doce magmatic arc in the Araçuaí-Ribeira boundary sector, southeast Brazil: Lithochemistry and isotopic (Sm–Nd and Sr) signatures', *Journal of South American Earth Science*, vol. 104, 102880, DOI:10.1016/j.jsames.2020.102880

Song, S.G., Wang, M.J., Wang, C. & Niu, Y.L. 2015, 'Magmatism during continental collision, subduction, exhumation and mountain collapse in collisional orogenic belts and continental net growth: A perspective', *China- Earth Science*, vol. 58, pp. 1284–1304, DOI:10.1007/s11430-015-5102-x

Sousa, C.S., Conceição, H., Soares, H.K., Fernandes, D.M. & Rosa, M.L.S. 2022, 'Magmatic processes recorded in plagioclase crystals of the Rio Jacaré Batholith, Sergipano Orogenic System, Northeast Brazil', *Journal of South American Earth Science*, vol. 118, 103942, DOI:10.1016/j.jsames.2022.103942

Streckeisen, F., 1976, 'Plutonic rocks, classification and nomenclature recommended by the IUGS subcommission on the Systematics of igneous Rocks', *Geotimes*, pp. 26-30, DOI:10.1007/BF01820841

Tedeschi, M., Novo, T., Pedrosa-Soares, A., Dussin, I., Tassinari, C., Silva, L.C., Gonçalves, L., Alkmim, F., Lana, C., Figueiredo, C., Dantas, E., Medeiros, S., De Campos, C., Corrales, F. & Heilbron, M. 2016, 'The Ediacaran Rio Doce magmatic arc revisited (Araçuaí-Ribeira orogenic system, SE Brazil)', *Journal of South American Earth Science*, vol. 68, pp. 167–186, DOI:10.1016/j.jsames.2015.11.011

Teixeira, P.A.D., Fernandes, C.M., Mendes, J.C., Medeiros, S.R. & Rocha, I.S.A. 2020, 'U-Pb LA-ICP-MS and geochemical data of the Alto Chapéu Pluton: contributions on bimodal post-collisional magmatism in the Araçuaí belt (SE Brazil)', *Journal of South American Earth Science*, vol. 103, pp. 1–18, DOI:10.1016/j.jsames.2011.03.003

Valeriano, C.M., Tupinambá, M., Simonetti, A., Heilbron, M., Almeida, J.C.H. & Eiraldo, L.G. 2011, 'U-Pb LA- MC-ICPMS geochronology of Cambro-Ordovician post-collisional granites of the Ribeira belt, southeast Brazil: Terminal Brasiliano magmatism in central Gondwana supercontinent', *Journal of South American Earth Science*, vol. 32, pp. 416–428, DOI:10.1016/j.jsames.2011.03.003

Valeriano, C.M., Mendes, J.C., Tupinambá, M., Bongiolo, E., Heilbron, M. & Junho, M.C.B. 2016, 'Cambro- Ordovician post-collisional granites of the Ribeira Belt, SE-Brazil: a case of terminal magmatism of a hot orogen', *Journal of South American Earth Science,* vol. 68, pp. 416–428, DOI:10.1016/j.jsames.2015.12.014

Vieira, V.S. 2015, 'Geologia e Recursos Minerais do Estado do Espírito Santo: texto explicativo do mapa geológico e de recursos minerais. Geologia e Recursos Minerais do Estado do Espírito Santo: texto explicativo do mapa geológico e de recursos minerais', CPRM, Belo Horizonte.

Wang, M., Song, S., Niu, Y & Su, L. 2014, 'Post-collisional magmatism: Consequences of UHPM terrane exhumation and orogen collapse, N. Qaidam UHPM belt, NWChina', *Lithos*, vol. 210–211, pp. 181–198, DOI:10.1016/j.lithos.2014.10.006

Wilson, J.T. 1966, 'Did the Atlantic close and re-open?', *Nature*, vol. 211, pp. 676-681

Whitney, D.L. & Evans, B.W. 2010, 'Abbreviations for names of rock-forming minerals', American Mineral. 95, 185–187, DOI:10.2138/am.2010.3371

Wiedemann, C.M., Medeiros, S.R., Ludka, I.P., Mendes, J.C. & Costa-de-Moura, J. 2002, 'Architecture of late orogenic plutons in the Araçuaí-Ribeira fold belt, southeast Brazil', *Gondwana Research*, vol. 5, pp. 381–399, DOI:10.1016/S1342-937X(05)70730-9

Wisniowski, L., Pedrosa-Soares, A. C., Medeiros-Junior, E., Belém, J., Dussin, I. & Queiroga, G. 2021, 'Ultra- high temperature, mid-crustal level, contact metamorphism imprinted on granulite facies paragneisses by a norite intrusion (São Gabriel da Baunilha, Araçuaí orogen, southeast Brazil)', *Journal of Metamorphic Geology*, vol. 39 (7), pp. 867–895, DOI:10.1111/jmg.12594

Yang, Q.Y., Ganguly, S., Shaji, E., Dong, Y. & Kumar, V.N. 2019, 'Extensional collapse of the Gondwana orogen: Evidence from Cambrian mafic magmatism in the Trivandrum Block, southern India', *Geoscience Frontiers*, pp. 263-284, DOI:10.1016/j.gsf.2017.12.002

Zanon, M. L., Chaves, A.O., Rangel, C.*V.G.* T., Gaburo, L. & Pires, C., R. 2015, 'Os aspectos geológicos do Maciço Santa Angélica (ES): uma nova abordagem', *Brazilian Journal of Geology*, vol. 45, no. 4, pp. 609-63, DOI:10.1590/2317-4889201520150005

Zhang, J., Wang, T., Castro, A., Zhang, L., Shi, X., Tong, Y., Zhang, Z., Guo, L., Yang, Q. & Iaccheri, L.M. 2016, 'Multiple Mixing and Hybridization from Magma Source to Final Emplacement in the Permian Yamatu Pluton, the Northern Alxa Block, China', *Journal of Petrology*, vol. 57, no. 5, pp. 933–980, DOI: 10.1093/petrology/egw028

Author contributions

Iago Mateus Lopes de Macêdo: conceptualization; formal analysis; methodology; validation; writing-original draft; writing – review and editing; visualization. Guilherme Loriato Potratz: methodology; validation. Marilane Gonzaga de Melo: methodology; validation; writing-original draft; writing – review and editing. Rodson de Abreu Marques: methodology; validation; writing-original draft; writing – review and editing Camila Cardoso Nogueira: review and editing; visualization. Werlem Holanda dos Santos: review and editing; visualization. Renzo Dias Rodrigues: review and editing; visualization. Mauro Cesar Geraldes: methodology; validation; writing-original draft; writing – review and editing

Conflict of interest

The authors declare no conflict of interest.

Data availability statement

The datasets generated and/or analyzed during the current study are fully available in the supplementary materials provided with this publication.

Funding information

The authors thank the funding agencies. Iago Mateus Lopes de Macêdo thanks Coordenação de Aperfeiçoamento de Pessoal de Nível Superior for doctoral process numbers 88887.601070/2021-00. Guilherme Loriato Potratz thanks Fundação Carlos Chagas Filho de Amparo à Pesquisa do Estado do Rio de Janeiro for his post doctoral scholarship, process numbers E26-204.530/2021 and E26-204.531/2021. Mauro Cesar Geraldes thanks the National Council for Scientific and Technological Development (CNPq) for the research grant (process nº 301470/2016-2).

How to cite:

Macêdo, I.M.L., Potratz, G.L., Melo, M.G., Marques, R.A., Nogueira, C.C., Santos, W.H., Rodrigues, R.D. & Geraldes, M.C. 2025, 'Petrogenesis of Cambro-Ordovician Magmatism in Araçuaí Orogen, SE Brazil: Petrography, Litogeochemistry and Zircon Geochronology of the Pedra Azul Intrusive Complex', *Anuário do Instituto de Geociências,* 48:66562. https://doi.org/10.11137/1982-3908_2025_48_66562